Multiplicity distributions from central collisions of ^{16}O+Cu at 14.6A GeV/c and intermittency

T. Abbott,[4,a] Y. Akiba,[7] D. Alburger,[2] D. Beavis,[2] P. Beery,[4] M. A. Bloomer,[10,b] P. D. Bond,[2] C. Chasman,[2] Z. Chen,[2] Y. Y. Chu,[2] B. A. Cole,[10,c] J. B. Costales,[10,d] H. J. Crawford,[3] J. B. Cumming,[2] R. Debbe,[2] E. Duek[2,e] J. Engelage,[3] S. Y. Fung,[4] L. Grodzins,[10] S. Gushue,[2] H. Hamagaki,[7] O. Hansen,[2,f] P. Haustein,[2] S. Homma,[7] H. Z. Huang,[10,g] Y. Ikeda,[8,h] J. Kang,[4,i] S. Katcoff,[2] S. Kaufman,[1] R. J. Ledoux,[10,d] M. J. Levine,[2] P. J. Lindstrom,[9] Y. Miake,[2,j] R. J. Morse,[10,b] S. Nagamiya,[5] J. Olness,[2] C. G. Parsons,[10,k] L. P. Remsberg,[2] H. Sakurai,[11] M. Sarabura,[10,l] R. Seto,[4] S. G. Steadman,[10] G. S. F. Stephans,[10] T. Sugitate,[6] M. Tanaka,[2] M. J. Tannenbaum,[2] M. Torikoshi,[7,m] J. H. van Dijk,[2] F. Videbæk,[1,n] M. Vient,[4,o] P. Vincent,[2,p] E. Vulgaris,[10,q] V. Vutsadakis,[10] W. A. Watson III,[2,r] H. E. Wegner,[2,s] D. S. Woodruff,[10] and W. A. Zajc[5]

(The E-802 Collaboration)

[1]*Argonne National Laboratory, Argonne, Illinois 60439*
[2]*Brookhaven National Laboratory, Upton, New York 11973*
[3]*University of California, Space Sciences Laboratory, Berkeley, California 94720*
[4]*University of California, Riverside, California 92507*
[5]*Columbia University, New York, New York 10027 and Nevis Laboratories, Irvington, New York 10533*
[6]*Hiroshima University, Hiroshima 730, Japan*
[7]*Institute for Nuclear Study, University of Tokyo, Tokyo 188, Japan*
[8]*Kyushu University, Fukuoka 812, Japan*
[9]*Lawrence Berkeley Laboratory, Berkeley, California 94720*
[10]*Massachusetts Institute of Technology, Cambridge, Massachusetts 02139*
[11]*Department of Physics, University of Tokyo, Tokyo 113, Japan*

(Received 2 June 1995)

The E-802 Collaboration at the BNL-AGS has measured charged particle multiplicity distributions from central (ZCAL) collisions of ^{16}O+Cu at 14.6A GeV/c as a function of the pseudorapidity interval $\delta\eta \geq 0.1$ in the range $1.2 \leq \eta \leq 2.2$. The fluctuations of these distributions as a function of the pseudorapidity interval have been studied by the method of normalized factorial moments and also by directly fitting the measurements to negative binomial distributions (NBD). Excellent fits to NBD were obtained in all $\delta\eta$ bins, allowing, for the first time, a systematic formulation of the subject of intermittency in terms of distributions to complement the description based on normalized factorial moments. In agreement with all previous measurements of NBD fits to multiplicity distributions in hadron and lepton reactions, the k parameter of the NBD fit for central ^{16}O+Cu collisions is found to exhibit an apparently linear increase with the $\delta\eta$ interval, albeit with a much steeper slope than for other reactions, and a nonzero intercept, $k(0) \neq 0$. The evolution of the NBD parameter $k(\delta\eta)$ is used to determine the two-particle short-range rapidity correlation length for central ^{16}O+Cu collisions, $\xi = 0.18 \pm 0.05$, which is much shorter than the value $\xi \sim 1-3$ for hadron collisions, but this is a quantitative rather than a qualitative difference. These results lead to a simple and elegant explanation of the

---

[a]Now at Reedley College, Reedley, CA 93654.
[b]Now at Lawrence Berkeley Laboratory, Berkeley, CA 94720.
[c]Now at Nevis Laboratories, Irvington, NY 10533.
[d]Now at Radionics Software Applications, Inc., Burlington, MA 01803.
[e]Now at New Side S.A., Buenos Aires, Argentina.
[f]Now at Niels Bohr Institute for Astronomy, Physics and Geophysics, DK-1200 Copenhagen Ø, Denmark.
[g]Now at Purdue University, West Lafayette, IN 47907.
[h]Now at Hitachi Limited, Hitachi, Ibaraki 316, Japan.
[i]Now at Yonsei University, Seoul, 120-749, Korea.
[j]Now at University of Tsukuba, Tsukuba, Ibaraki 305, Japan.
[k]Now at NITON, Bedford, MA 01730.
[l]Now at 24B Bigelow St., Cambridge, MA 02139.
[m]Now at Mitsubishi Electric Co., Hyogo 652, Japan.
[n]Now at Brookhaven National Laboratory, Upton, NY 11973.
[o]Now at UC Irvine, Irvine, CA 92717.
[p]Now at Bruker Inc., Karlsruhe, Germany.
[q]Now at Bell Telephone Laboratory, Naperville, IL 60566.
[r]Now at CEBAF, Newport News, VA 23606.
[s]Deceased.

intermittency formalism, without resort to fractals, for all reactions, which demystifies intermittency—for ^{16}O+Cu central collisions, intermittency is nothing more than the apparent statistical independence of the multiplicity in small pseudorapidity bins, $\delta\eta\sim 0.2$, due to the surprisingly short two-particle rapidity correlation length.

PACS number(s): 25.75.+r, 13.85.Hd

I. INTRODUCTION

The concept of "intermittency" was introduced by Bialas and Peschanski [1] to try to explain the "large" fluctuations of multiplicity in restricted intervals of rapidity or pseudorapidity [2,3]. A formalism was proposed [1] to study nonstatistical (more precisely, non-Poisson) fluctuations as a function of the size of rapidity interval, and it was further suggested [1] that the "spikes" in the rapidity fluctuations were evidence of fractal or intermittent behavior, in analogy to turbulence in fluid dynamics which is characterized by self-similar fluctuations at all scales—the absence of a well-defined scale of length [4]. Bialas and Peschanski proposed that the data be presented as normalized factorial moments of order q:

$$F_q(\delta\eta)=\frac{\langle n(n-1)\cdots(n-q+1)\rangle}{\langle n\rangle^q}, \tag{1}$$

where n is the multiplicity in a pseudorapidity interval (bin) of size $\delta\eta$ on a given event and the angular brackets indicate averaging over all events. Intermittency would be indicated by a power-law increase of multiplicity distribution moments over pseudorapidity bins as the bin size is reduced:

$$F_q(\delta\eta)\propto(\delta\eta)^{-\phi_q}. \tag{2}$$

The normalized factorial moment with the clearest interpretation is

$$F_2=\frac{\langle n(n-1)\rangle}{\langle n\rangle^2}=\frac{\langle n^2\rangle-\langle n\rangle}{\langle n\rangle^2}=\frac{\sigma^2+\langle n\rangle^2-\langle n\rangle}{\langle n\rangle^2}$$
$$=1+\frac{\sigma^2}{\mu^2}-\frac{1}{\mu}, \tag{3}$$

where $\mu\equiv\langle n\rangle$ is the mean and $\sigma\equiv\sqrt{\langle n^2\rangle-\langle n\rangle^2}$ is the standard deviation. Note that the normalized factorial moments are all equal to unity for a Poisson distribution.

The formulation of this new concept of intermittency in terms of moments was taken by many as a partially retrograde development, particularly since the greatest advance in multiplicity distributions in 20 years had recently been made by the UA5 Collaboration [5] who actually determined the functional form of multiplicity distributions. The negative binomial distribution (which had been used sporadically for the total multiplicity [6]) was used by the UA5 Collaboration [7] as a "remarkable" description of their measured multiplicity distributions in intervals of rapidity which are not significantly constrained by conservation laws [8–11] and also for the total multiplicity. Also, a related distribution, the gamma distribution, had been used to describe E_T distributions [12]. One could not help but wonder what intermittent behavior would look like in terms of distributions rather than moments—since once the distribution is known, then all the moments are known.

An intermittency analysis of charged particle multiplicity data from central collisions of ^{16}O+Cu at 14.6A GeV/c by the method of normalized factorial moments has been published by the AGS-E802 Collaboration [13]. In agreement with previous measurements [14], an apparent power-law growth of moments with decreasing pseudorapidity interval was observed in the range $1.0\geq\delta\eta\geq 0.1$. In the present work, multiplicity distributions in individual pseudorapidity bins are presented for the same data. These distributions are excellently fit by negative binomial distributions (NBD's) in all $\delta\eta$ bins, allowing, for the first time, a systematic formulation of the subject of intermittency in terms of distributions to complement the normalized factorial moment analysis. The two parameters of the NBD fit which characterize the shape of the distribution and its deviation from a Poisson are determined as a function of the pseudorapidity interval $\delta\eta$. The evolution with $\delta\eta$ of the NBD parameters will be seen to yield a simple and elegant explanation of the intermittency phenomenology in terms of the mainstream of multiparticle physics of the past decades, namely, the two-particle short-range rapidity correlation length [15,9,16–19]. The key to this understanding of intermittency, which has not previously been clear, is a dramatic reduction of the two-particle rapidity correlation length for ^{16}O+Cu central collisions from the value in hadron-hadron collisions [15]. Moreover, the correlation length for central ^{16}O+Cu collisions, although smaller than expected, is quite finite and can be measured—which means that a length scale exists in these collisions and therefore there is no intermittency [1,4] in the multiplicity fluctuations. The weakened, but still finite, short-range rapidity correlations in collisions of relativistic heavy ions had been predicted [17,18,20,21], since the conventional short-range correlations should be washed out by the random superposition of correlated sources [18,22,23], so that eventually only the quantum-statistical Bose-Einstein (BE) correlations should remain [17,18,24].

The organization of this paper is as follows. The next section describes some details of the experiment. In Sec. III, the analysis of the data by the method of normalized factorial moments is reviewed, while in Sec. IV, multiplicity distributions from the same data set are presented. In Sec. V, the relevant properties of the negative binomial and gamma distributions are briefly noted. Section VI presents fits to the measured multiplicity distributions, and in Sec. VII, the results of the fits are used to describe the systematics of multiplicity distributions and to relate these to the intermittency phenomenology. In Sec. VIII, the formalism of multiparticle correlations and Mueller moments is reviewed, leading to Sec. IX in which the evolution of the NBD parameter with $\delta\eta$ is quantitatively related to the two-particle short-range

rapidity correlation. Correction of the data for instrumental effects is discussed in Sec. X, with the final results for the two-particle rapidity correlation length and strength presented in Sec. XI. Related measurements are discussed in Sec. XII, while the results and conclusions of the present work are summarized in Sec. XIII.

II. SOME DETAILS OF THE EXPERIMENT

The data presented in this report come from BNL experiment E802 using relativistic heavy ion beams available at the Tandem-AGS facility. A detailed description of the full E802 setup has been published [25], and so only the detector system relevant to this measurement will be discussed here. The Target Multiplicity Array (TMA) measures the production angles of charged particles in the pseudorapidity range $-1.2<\eta<3.1$ with almost full coverage in azimuthal angle ϕ; the primary gap in ϕ coverage is due to a small opening in the forward region to minimize the amount of material between the target and the E802 spectrometer. The TMA consists of resistive plastic tubes operated in the proportional mode and read out from image signals induced on cathode pads. There are 3240 pads in total and their sizes vary to ensure a nearly uniform occupancy rate. In order to eliminate electrical cross talk over tube boundaries, thin copper grounding strips are located between the tubes. These strips are electrically connected to ground via conducting silver paint and act as local rf shields which prevent pads from detecting signals on adjacent wires. It is still possible, however, to observe some small amount of cross counting over tube boundaries when particle tracks actually cross onto adjacent wires. This can occur because the detector is made of individual small panels which are slightly tilted so that tracks have non-normal incidence to avoid inefficiency due to the walls of the tubes. Such cross counting has been studied extensively and will be discussed in more detail below. The use of proportional tubes with pad readout can produce another type of cross talk which occurs between adjacent pads along the same tube: When two adjacent pads fire, it is impossible to determine whether a single charged particle passed between the two pads, inducing signals on both, or whether two distinct particles caused the signals. To address this problem, a conservative TMA counting convention was adopted: During data analysis, two clusters along a wire are always treated as a single particle passing through local regions between the adjacent pads. Monte Carlo simulations indicate that this convention is correct for over 88% of two-cluster signals [26] in ^{16}O+Cu central collisions. In the remaining 12% of cases, however, one or more nearby tracks are lost; these losses will of course tend to reduce the measured strength of any highly localized fluctuations in the charged particle density. Taking all cases into account, the estimated [26] loss of tracks due to multiple hits is $\leq 1\%$ for the present analysis.

The uniformity and efficiency of the detector were assured by constant monitoring. Hit distributions on individual pads and the ratio of double to single clusters along a wire were closely monitored on a run-by-run basis. Hot and "warm" pads as well as dead pads were all treated as malfunctioning and removed from the data. The uniformity of response was further checked by using the symmetry of the detector geometry to verify that azimuthally symmetric elements gave identical hit distributions to within the excellent statistics on each run, typically ~ 1000 hits per pad [26].

The reaction ^{16}O+Cu was chosen for the analysis of central collisions at 14.6A GeV/c to reduce multihit losses in the TMA detector and to minimize the ratio of target spectator protons to produced particles. Information provided by the E802 Zero-Degree Calorimeter (ZCAL) [25,27] was used to require the forward-going kinetic energy to be less than that of a single projectile nucleon (13.6 GeV). This cut, demanding that little or no kinetic energy remain in the projectile spectator region, served as the primary criterion for centrality. From a nuclear geometry calculation [28], only 3.2% of ^{16}O+Cu minimum bias events would be expected to pass this cut. The number of events in the sample passing the centrality cut was 20 994; thus these data correspond to approximately 0.6×10^6 ^{16}O+Cu interactions. For the present measurement, restrictions were placed on which hits in the TMA detector were accepted for analysis. Because of the spectrometer opening and some malfunctioning tubes, an azimuthal angle cut of $40°<\phi<240°$ was applied. The analysis was also restricted to those tracks falling in the pseudorapidity range $1.2\leq\eta\leq 2.2$. This range includes the peak in the pseudorapidity density and is in the region where the detector segmentation, angular resolution, and detection efficiency are high and nearly uniform. Within these intervals, the detector had approximately 1250 pads with a hardware inefficiency of 6% (mostly due to malfunctioning pads) and an average resolution of $\sigma_\eta\sim 0.025$ in η and $\sigma_\phi\sim 0.027$ rad in ϕ. After including multiple scattering (mostly from the target), overall resolutions are $\sigma_\eta\sim 0.03$ and $\sigma_\phi\sim 0.034$ for the ^{16}O+Cu system. These restrictions reduced the number of events in the sample to 19 667.

III. METHOD OF NORMALIZED FACTORIAL MOMENTS

The E802 intermittency analysis using the formalism of moments starts with the multiplicity in a large interval, $1.2\leq\eta\leq 2.2$, $\Delta\eta=1.0$, for which the evolution of the moments is determined as the interval is subdivided into M equal subintervals (bins). The normalized factorial moments, using "vertical" analysis, of order q are defined as [1,17,29]:

$$F_q^V=\frac{1}{M}\sum_{m=1}^{M}\frac{\langle k_m(k_m-1)\cdots(k_m-q+1)\rangle}{\langle k_m\rangle^q}. \tag{4}$$

M is the number of bins of size $\delta\eta=\Delta\eta/M$ into which the large pseudorapidity interval is divided, k_m is the multiplicity in the mth bin, and $\langle k_m\rangle$ is the event-averaged multiplicity in the mth bin. [This formulation is more complicated than that sketched in Eq. (1) which described a single bin of variable width $\delta\eta$.] Recall that $F_q\equiv 1$ for a Poisson distribution. Note that the factorial moments of order q are designed to emphasize "spikes," since bins with multiplicities less than q do not contribute to the numerator of Eq. (4). However, bins of all multiplicities, including empty bins, must be explicitly included in the calculation of the denominator in order to obtain the correct value for the average multiplicity. The measured moments of order 2–6 for ^{16}O+Cu central collisions are plotted in Fig. 1(a). As shown by the solid fitted lines, a linear increase of $\ln(F_q)$ with increasing

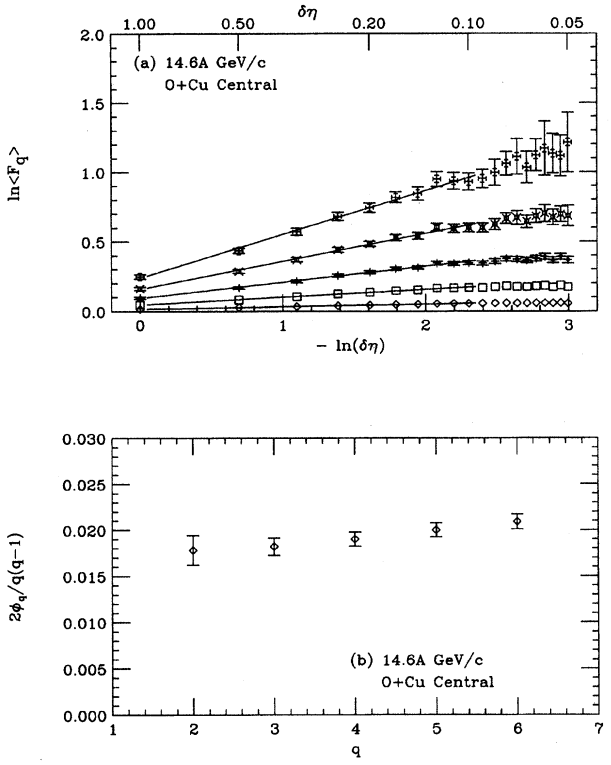

FIG. 1. (a) Normalized factorial moments F_q for central collisions of ^{16}O+Cu, for orders $q=2,3,4,5,6$, as a function of the pseudorapidity subinterval $\delta\eta$, presented as $\ln(F_q)$ versus $-\ln(\delta\eta)$. For each order, the lines represent power-law fits to the moments over the range $1.0\geq\delta\eta\geq 0.1$. As shown in (b), the increase of the power-law slopes ϕ_q with the order q follows the scaling law $2\phi_q/q(q-1)$.

$-\ln(\delta\eta)$ down to $\delta\eta=0.1$ is observed for all orders q. Thus, over the range $1.0\geq\delta\eta\geq 0.1$, the moments for each order exhibit a power law with constant slope, $\phi_q=-d(\ln F_q)/d(\ln\delta\eta)$, which increases with increasing order. Beyond $\delta\eta=0.1$, the slopes tend to roll over towards zero, especially for the low-order moments. Such slope changes at finer subintervals could be attributed to the effect of finite detector resolution and segmentation [13]. In Fig. 1(b), the slope parameters of the power-law fit are presented in terms of a moments scaling rule

$$\phi_q=\frac{q(q-1)}{2}\phi_2, \tag{5}$$

which they appear to follow to an excellent approximation. This scaling rule was proposed by Bialas and Peschanski [1] and was derived in the limit of a large number of cascade steps in their α model of intermittency. This behavior was also observed in other experiments [30–32] and commented upon by several authors [18,24,23]. Note that the slope parameters are very small, $\phi_2\simeq 0.018\ll 1$.

Care must be taken in interpreting these results since it will be shown that the values of the normalized factorial moments and the slope parameters are very sensitive to the instrumental effects of Dalitz decays, γ conversions, cross talk, occupancy, and single-track and two-track resolutions, for which explicit corrections have not yet been applied. The corrections will be discussed later. Yet much can be learned about the intermittency phenomenology by using the multiplicity distributions from the same data set to analyze the fluctuations directly.

IV. MULTIPLICITY DISTRIBUTIONS

The AGS-E802 multiplicity distributions for central collisions of ^{16}O+Cu at 14.6A GeV/c are shown in Fig. 2 in increasing intervals of pseudorapidity $\delta\eta=0.1,0.2,0.3,\ldots,0.8,0.9,1.0$ around a central value of $\eta=1.7$, where the bin of 1.0 covers $1.2\leq\eta\leq 2.2$ in the laboratory and is identical to the large $\Delta\eta=1.0$ interval of the moment analysis. Note that apart from the large interval, the data are not strictly identical for the two analyses since the momenta analysis averages over all M bins of size $\delta\eta=1.0/M$ in the interval $1.2\leq\eta\leq 2.2$, while the distributions are obtained only for bins of increasing size (full width) $\delta\eta$ about the center of the interval. The multiplicity distributions are shown in Fig. 2 as frequency distributions of the number of events with multiplicity n in an interval of size $\delta\eta$ for the

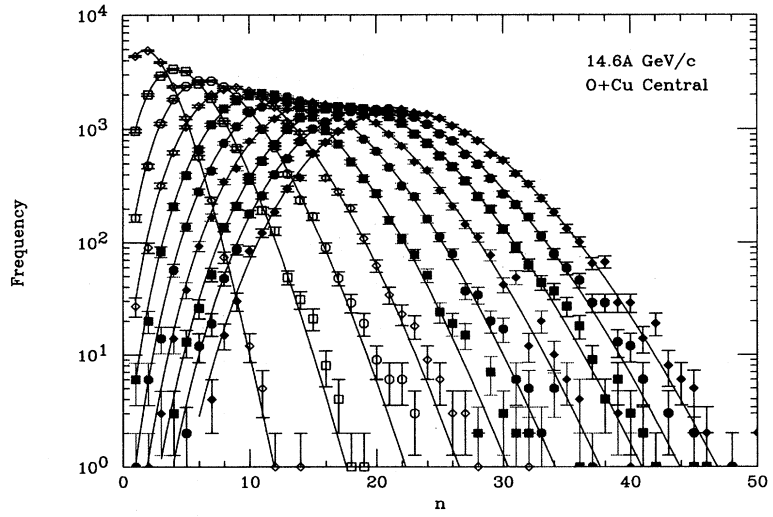

FIG. 2. Multiplicity distributions for ^{16}O+Cu central collisions at 14.6A GeV/c presented as frequency distributions of the number of events with multiplicity n in a pseudorapidity interval of full width $\delta\eta=0.1,0.2,0.3,\ldots,0.8,0.9,1.0$ centered at laboratory pseudorapidity $\eta=1.7$. The solid lines connect data points from the same $\delta\eta$ bin.

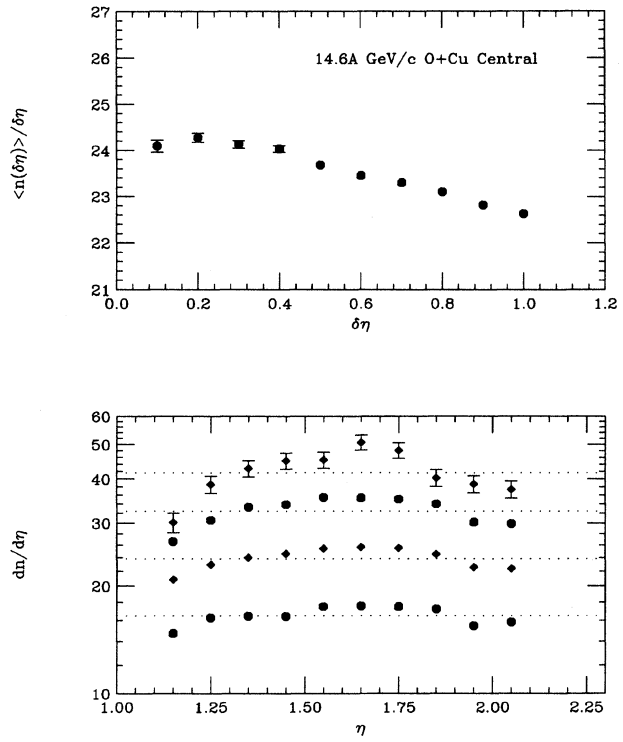

FIG. 3. (a) $\langle dn/d\eta \rangle$ averaged over the bins of $\delta\eta$ presented as $\langle n(\delta\eta)\rangle/\delta\eta$ as a function of $\delta\eta$. (b) The differential pseudorapidity distribution $dn/d\eta$ of multiplicity in the interval $1.2 \leq \eta \leq 2.2$ for slices of multiplicity n in this interval in the range 10−19, 20−29, 30−39, and 40−49. The dotted lines show the average multiplicity for each slice.

ten intervals. For each $\delta\eta$, the distributions all have the same number of events, 19 667. The solid lines on the figure are to help guide the eye to the data points from the same $\delta\eta$ bin—however, they also represent NBD fits to the distributions which will be discussed, extensively, in due course. The average multiplicities in the subintervals $\langle n(\delta\eta)\rangle$ increase rather linearly with the widths of the subintervals, indicating that the pseudorapidity density of the average multiplicity $\langle dn/d\eta \rangle$ for these data is reasonably constant (2.5% rms variation) over the large interval $1.2 \leq \eta \leq 2.2$. A slight deviation from linearity can be seen by presenting the data in the form $\langle n(\delta\eta)\rangle/\delta\eta$ versus $\delta\eta$ [Fig. 3(a)] where a systematic increase of $\langle n(\delta\eta)\rangle/\delta\eta$ is visible toward the smallest bins, near the center of the large interval ($\eta \simeq 1.7$). There is concern that this peaking could be indicative of a narrowing of the width of the pseudorapidity distribution with increasing multiplicity [33]. To investigate this possibility, a plot was made [see Fig. 3(b)] of the differential pseudorapidity distribution $dn/d\eta$ of multiplicity in the interval $1.2 \leq \eta \leq 2.2$ for slices of multiplicity in this interval in the range 10–19, 20–29, . . . ,40–49, which covers essentially the whole range of multiplicities in this interval ($\delta\eta = 1.0$, Fig. 2). The dotted lines in Fig. 3(b) show the average multiplicity for each slice. The central values of the distributions are 10%–20% above the average values, and likewise the wings of the distributions are below the averages. Hence, there is no evidence for any change in shape of the $dn/d\eta$ distribution with multiplicity. Thus it is also to be expected that differences in the moment and distribution analyses resulting from averaging over the whole $\Delta\eta$ interval or only over the central parts of the interval with increasing $\delta\eta$ should be minimal.

In Fig. 4, the multiplicity distributions of Fig. 2 from selected subintervals are presented in the form scaled by the mean $\langle n \rangle$ in each case to emphasize the evolution of the shape of the distributions with increasing pseudorapidity interval $\delta\eta$. These data are reminiscent of the original discovery by UA5 [2,5] that multiplicity distributions in restricted intervals of pseudorapidity exhibit large fluctuations about the average which favor higher multiplicity and that these fluctuations increase with decreasing pseudorapidity interval $\delta\eta$. However, by comparison, the present data are particularly striking in that the shape of the multiplicity distribution changes from nearly exponential to nearly Gaussian over a small range of pseudorapidity, less than one unit.

It should be noted that the exact details of the centrality cut are important for the shapes of the distributions in Fig. 4 and for the analysis by moments. The shapes of the distributions below the mean value are determined by the centrality cut. For the present analyses, the ZCAL was used to define

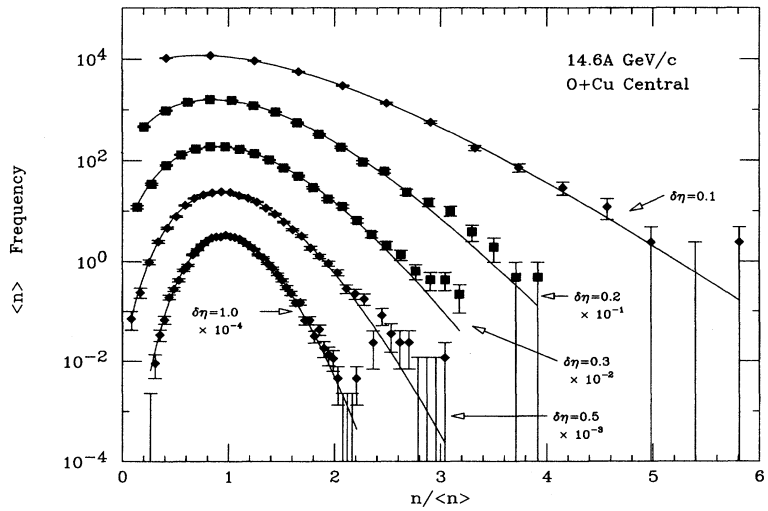

FIG. 4. Multiplicity distributions from Fig. 2 for the $\delta\eta$ intervals 0.1,0.2,0.3,0.5.1.0, as indicated. The data for each interval are plotted scaled in multiplicity by $\langle n \rangle$, the mean multiplicity in the interval. Each successive distribution has been normalized by the factor indicated, for clarity of presentation.

centrality—by the requirement that the forward-going kinetic energy be less than that of a single projectile nucleon (13.6 GeV), corresponding to 3.2% of minimum bias interactions—which is an indirect cut on multiplicity. The usual centrality definition by a sharp cut on the multiplicity itself—typically, at an upper percentile [34] of 7%—would have caused the distributions to be severely truncated, which would obviously also have caused severe distortions in the moments [35]. The ZCAL centrality cut gives smooth distributions which vary uniformly with $\delta\eta$.

V. NEGATIVE BINOMIAL AND GAMMA DISTRIBUTIONS

Before a detailed discussion can be made of the shapes of these multiplicity distributions and their fluctuations, it is worthwhile to review some properties of the negative binomial and gamma distributions. These distributions have distinct—and in some cases "counterintuitive"—properties compared to the Poisson distribution which forms the basis of "intuition" on counting statistics. The Poisson distribution is intimately linked to the exponential law of radioactive decay of nuclei [36,37], the time distribution of nuclear disintegration counts, giving rise to the common usage of the term [36] "statistical fluctuations" to describe the Poisson statistics of such counts. The Poisson distribution results from repeated independent trials, each with the same probability for a given outcome—if the probability of the outcome varies or if any correlation is introduced so that the trials are not independent, the distribution tends to become negative binomial [38].

The negative binomial distribution of an integer m is defined as

$$P(m)=\frac{(m+k-1)!}{m!(k-1)!}\frac{(\mu/k)^m}{(1+\mu/k)^{m+k}}, \tag{6}$$

where $P(m)$ is normalized for $0\leq m\leq\infty$, $\mu\equiv\langle m\rangle$, and some higher moments are

$$\sigma=\sqrt{\mu\left(1+\frac{\mu}{k}\right)}, \quad \frac{\sigma^2}{\mu^2}=\frac{1}{\mu}+\frac{1}{k}, \quad F_2=1+\frac{1}{k}. \tag{7}$$

The normalized factorial moments (F_q) and normalized factorial cumulants (K_q) [39,40] of the NBD are particularly simple:

$$F_q=F_{(q-1)}\left(1+\frac{q-1}{k}\right), \quad K_q=\frac{(q-1)!}{k^{q-1}}. \tag{8}$$

The NBD, with an additional parameter k compared to a Poisson distribution, becomes Poisson in the limit $k\to\infty$ and binomial for k equal to a negative integer (hence the name). The extra parameter has made the NBD useful to mathematical statisticians as a test for whether a distribution is Poisson—more precisely as a "test for independence in rare events" [38]. The test for a Poisson distribution consists of determining whether the NBD parameter $1/k$ is consistent with zero to within its error $s_{1/k}$, which is given [38] as

$$s_{1/k}=\frac{s_k}{k^2}=\frac{1}{\mu}\sqrt{\frac{2}{N}}, \tag{9}$$

where N is the total number of events. For statisticians, the NBD represents the first departure from a Poisson law. Physicists are more likely to describe the NBD as Bose-Einstein ($k=1$) or generalized Bose-Einstein $k\neq 1$ distributions [6].

The negative binomial distribution bears a strong relationship to the gamma distribution and becomes a gamma distribution in the limit $\mu\gg k>1$. In fact, many times, gamma distributions are substituted for NBD to prove various theorems [41]. The gamma distribution represents the probability density for a continuous variable x and has a parameter p:

$$f(x)=\frac{b}{\Gamma(p)}(bx)^{p-1}e^{-bx}, \tag{10}$$

where

$$p>0, \quad b>0, \quad 0\leq x\leq\infty.$$

$\Gamma(p)=(p-1)!$ if p is an integer, and $f(x)$ is normalized. The first few moments of the distribution are

$$\mu\equiv\langle x\rangle=\frac{p}{b}, \quad \sigma=\frac{\sqrt{p}}{b}, \quad \frac{\sigma^2}{\mu^2}=\frac{1}{p}, \quad F_2-1=\frac{(1-b)}{p}. \tag{11}$$

One important difference between NBD and gamma distributions is in the limit m or $x\to 0$: For $p>1$ the limit is always zero for a gamma distribution, whereas for the NBD it is always finite.

The gamma distribution has an important property under convolution. Define the n-fold convolution of a distribution with itself as

$$f_n(x)=\int_0^x dy\, f(y)f_{n-1}(x-y) \ ; \tag{12}$$

then, for a gamma distribution [Eq. (10)], the n-fold convolution is simply given by the function

$$f_n(x)=\frac{b}{\Gamma(np)}(bx)^{np-1}e^{-bx} \ ; \tag{13}$$

i.e., $p\to np$ and b remains unchanged. Notice that the mean μ_n and standard deviation σ_n of the n-fold convolution obey the familiar rule

$$\mu_n=n\mu, \quad \sigma_n=\sigma\sqrt{n}. \tag{14}$$

The convolution property of the gamma distribution also holds for the NBD. The probability distribution of the sum of n independent variables, each distributed as a NBD with mean μ and parameter k, is the n-fold convolution of the distribution, which is a NBD with mean $n\mu$ and parameter nk, so that the ratio μ/k remains constant for the convolutions exactly like the gamma distribution. Furthermore, the familiar rule for the mean and standard deviation [Eq. (14)] is satisfied.

An important difference in the properties of the NB and Poisson distributions is related to convolutions and concerns the random decomposition of a distribution from a large interval onto smaller subintervals. Suppose the population on a

TABLE I. Results of NBD fits to ^{16}O+Cu multiplicity distributions.

$\delta\eta$	$\langle n\rangle,(\sigma)$ Data	$\mu,(\sigma)$ Fit	k	N_0 Data	N_0 Fit	χ^2/N_{DF}
0.1	2.69 (1.53)	2.41 (1.66)	16.35±1.7	17622	19704	5.1/11
0.2	4.92 (2.40)	4.86 (2.44)	21.37±1.3	19456	19705	30/16
0.3	7.24 (3.02)	7.24 (3.03)	27.04±1.3	19643	19676	39/20
0.4	9.62 (3.52)	9.61 (3.52)	33.65±1.5	19662	19666	46/29
0.5	11.84 (3.96)	11.84 (3.94)	37.52±1.6	19666	19667	44/33
0.6	14.08 (4.34)	14.07 (4.34)	41.8±1.7	19667	19667	42/34
0.7	16.32 (4.70)	16.31 (4.69)	46.8±1.8	19667	19667	59/37
0.8	18.48 (5.01)	18.48 (5.00)	52.1±2.0	19667	19667	39/41
0.9	20.52 (5.29)	20.54 (5.28)	57.1±2.2	19667	19667	47/42
1.0	22.63 (5.53)	22.60 (5.53)	64.4±2.5	19667	19669	63/42

large interval, e.g., $\Delta\eta=1$, follows the NBD, and the population is subdivided randomly by repeated independent trials onto a smaller subinterval, e.g., $\delta\eta$, with constant probability ζ per trial—this is actually a binomial decomposition of the original population into two subpopulations on the subintervals ζ and $1-\zeta$. The populations on the two subintervals are also negative binomial distributed [42,43], with means $\zeta\mu$ and $(1-\zeta)\mu$ and the same parameter k [43,44]. Note, however, that any clustering (i.e., correlation among the trials) would cause k to vary [45]. Most importantly, and the principal distinguishing characteristic of the NBD compared to a Poisson, the populations on the two subintervals are *not* statistically independent—the distribution on one subinterval depends explicitly on the result on the other subinterval—so that the distributions on the two subintervals cannot be convoluted to recover the original distribution on the large interval. This characteristic property of the negative binomial distribution has important physical consequences, forward-backward (long-range) multiplicity correlations [46,5–7]—the mean backward multiplicity is linearly proportional to the forward multiplicity. Also, the fact that k remains constant for a binomial decomposition of a NBD gave rise to the expectation [43,44] that k should remain constant (i.e., independent of the size of the pseudorapidity interval) in relativistic heavy ion collisions.

VI. FITS TO THE MULTIPLICITY DISTRIBUTIONS

The multiplicity distributions from Fig. 2 have been fit to both negative binomial and gamma distributions. The results are given in Tables I and II and shown for the $\delta\eta=0.2,0.5,1.0$ intervals in Figs. 5(a), 5(b). The NBD provides an excellent fit to both the rising and falling parts of the distributions, although it tends to be slightly low in the upper tails. The gamma distribution is low in the rising part of all the distributions and tends to be above the data in the upper tails. It is worth pointing out that the fits are performed using a maximum likelihood method with the assumption of Poisson fluctuations of the data points around the expected (best fit) frequency of events with observed multiplicity n in a pseudorapidity bin $\delta\eta$. The fact that the NBD fits exhibit acceptable $\chi^2\simeq 1$ per degree of freedom for all $\delta\eta$ bins means that the deviations of the data points from the curves in Fig. 5(a) are indeed consistent with *statistical fluctuations*. For the gamma distribution fits, the $\chi^2\sim 3$–20 per degree of freedom are unacceptably high and reflect the small but statistically significant systematic deviation of the curves from the data in Fig. 5(b). The advantage of using the Poisson maximum likelihood method instead of fits which minimize χ^2 is that the cases with zero or small numbers of observed events are correctly treated. This results in the excellent agreement of the data and the fit for N_0, the total number of events in each plot, and for the means and standard deviations of the distributions. The only disagreement is in the smallest $\delta\eta$ intervals where in fact the values labeled "N_0 data" in Tables I and II are incorrect because events with $n(\delta\eta)=0$ are not included in the distributions and thus are missing form the sum of the data (although they are accounted for correctly in the moment analysis).

TABLE II. Results of gamma fits to ^{16}O+Cu multiplicity distributions.

$\delta\eta$	$\langle n\rangle$ Data	μ Fit	b	p	N_0 Data	N_0 Fit	χ^2/N_{DF}
0.1	2.69	2.67	1.07±0.02	2.86±0.04	17622	17783	87/11
0.2	4.92	4.90	0.79±0.01	3.87±0.04	19456	19448	336/16
0.3	7.24	7.24	0.73±0.008	5.29±0.05	19643	19648	275/20
0.4	9.63	9.58	0.73±0.007	6.99±0.06	19662	19662	237/29
0.5	11.84	11.83	0.72±0.007	8.52±0.08	19666	19666	211/32
0.6	14.08	14.17	0.71±0.007	10.06±0.10	19667	19669	158/34
0.7	16.32	16.41	0.71±0.007	11.65±0.12	19667	19669	157/37
0.8	18.48	18.39	0.72±0.007	13.24±0.13	19667	19668	92/41
0.9	20.52	20.39	0.72±0.007	14.68±0.15	19667	19668	126/42
1.0	22.63	22.69	0.72±0.007	16.34±0.16	19667	19668	111/42

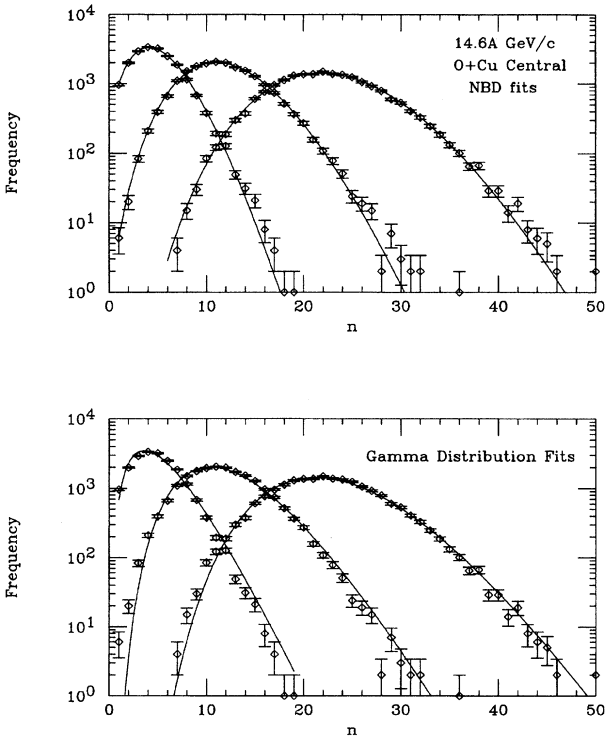

FIG. 5. Multiplicity distributions from the intervals $\delta\eta=0.2,0.5.1.0$ together with the results of the fits: (a) negative binomial distribution, (b) gamma distribution. The best fit parameters are given in Tables I and II.

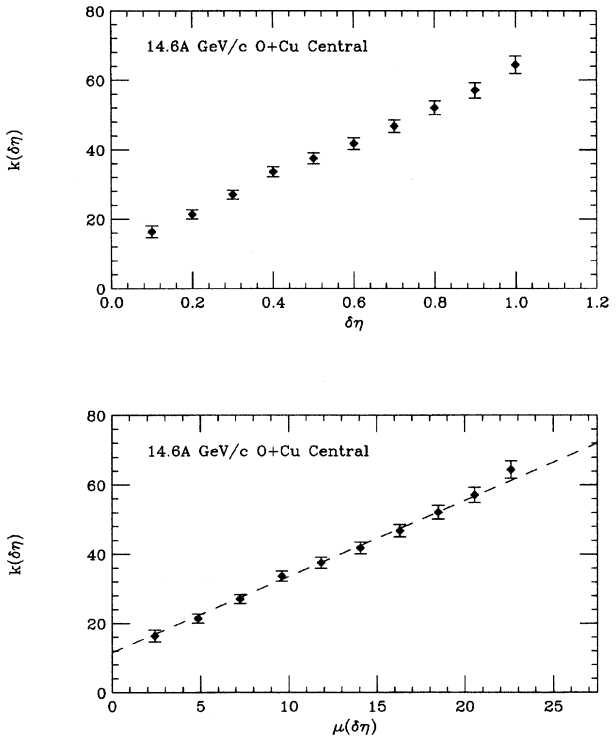

FIG. 6. $k(\delta\eta)$ parameter from NBD fits to the data as a function of (a) the interval $\delta\eta$, (b) the average multiplicity in the interval $\mu(\delta\eta)=\langle n(\delta\eta)\rangle$. The dashes represent the linear relationship discussed in the text.

It is worth reiterating that the exact details of the centrality cut are important for Figs. 2 and 5 since the rising (lower multiplicity) parts of the distributions are determined by the centrality cut. The excellence of the fits of the NBD to the rising as well as the falling parts of all the distributions is attributed to use of the ZCAL centrality cut, which is an indirect cut on multiplicity, rather than the sharp cut on multiplicity which is traditionally used to define centrality. This leads to the speculation that the ZCAL requirement that all the projectile nucleons interact may, in fact, produce a well defined final state with real physical meaning, in distinction to many of the other methods of defining central collisions.

VII. SYSTEMATICS OF THE DISTRIBUTIONS AND INTERMITTENCY

The k parameters of the NBD fits are plotted in Fig. 6 and show a totally unexpected, strikingly steep, *linear* increase with the width and mean multiplicity $[\mu=\langle n(\delta\eta)\rangle]$ of the interval—k varies by more than a factor of 3 over 1 unit of $\delta\eta$. This is in sharp contrast to the UA5 results [5], where k is also linear with $\delta\eta$ but varies by only $\sim 10\%$ over the same interval. A similar effect is seen (Fig. 7) for the evolution of the $p(\delta\eta)$ parameter of the gamma distribution fits; however, a clear nonlinearity is visible near $\delta\eta=0$. This might be attributed to the inadequacy of the gamma distribution for arguments near zero—or it may be more fundamental. Particularly noteworthy for the gamma distribution (Table II) is that for $\delta\eta\geq 0.3$, the fitted values of b are all constant to within $\sim 1\%$. Since $b=p/\mu$, this means that the values of $p(\delta\eta)$ increase linearly with $\mu(\delta\eta)$—in direct proportion to within 1%—a characteristic signature of convolutions [Eq. (13)]. This seems to imply that the multiplicities added by each incremental increase of the width of the $\delta\eta$ interval combine as if they were statistically independent variables. From Tables I and II, it can be seen that the ratio $k(\delta\eta)/\mu(\delta\eta)$ for the NBD fits is not nearly so constant as $p(\delta\eta)/\mu(\delta\eta)$. However, it is evident from Fig. 6 that this is merely the result of the nonzero intercept, $k(0)\neq 0$, for the strikingly linear dependence of $k(\delta\eta)$ on $\mu(\delta\eta)$ from the NBD fits.

Just as the linear increase of $k(\delta\eta)$ or $p(\delta\eta)$ with the width of the interval $\delta\eta$ is an indication that the multiplicities added in each increment of $\Delta(\delta\eta)\sim 0.1$ act as if they were statistically independent variables, the relatively constant value of $p(\delta\eta)$ in the two lowest bins, and perhaps the finite intercept $k(0)\neq 0$, is reminiscent of the property of the sum of 100% correlated variables. Thus it is tempting to interpret the sharply rising increase of $k(\delta\eta)$ with $\delta\eta$ as evidence of a random component of multiplicity, and the nonzero intercept, $k(0)\neq 0$, as an indication of correlations at small $\delta\eta$. The dramatically different rate of increase of $k(\delta\eta)$ with $\delta\eta$ for the present data compared to the UA5 data [5] would then be taken as an indication that the relative balance of randomness and correlation is considerably different for the two cases. In fact, such considerations can be put on a mathematical basis for any degree of correlation, as will be discussed below (Sec. IX).

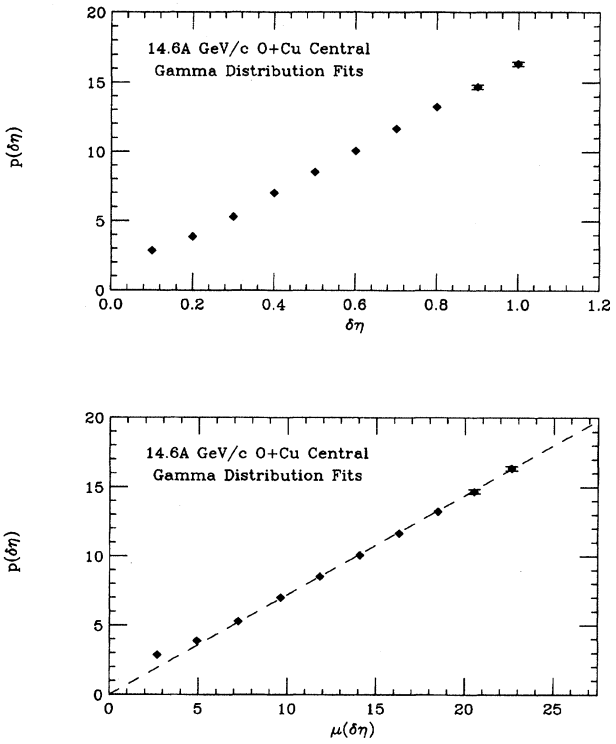

FIG. 7. $p(\delta\eta)$ parameter from gamma distribution fits to the data as a function of (a) the interval $\delta\eta$, (b) the average multiplicity in the interval $\mu(\delta\eta)=\langle n(\delta\eta)\rangle$. The dashes represent the linear relationship discussed in the text.

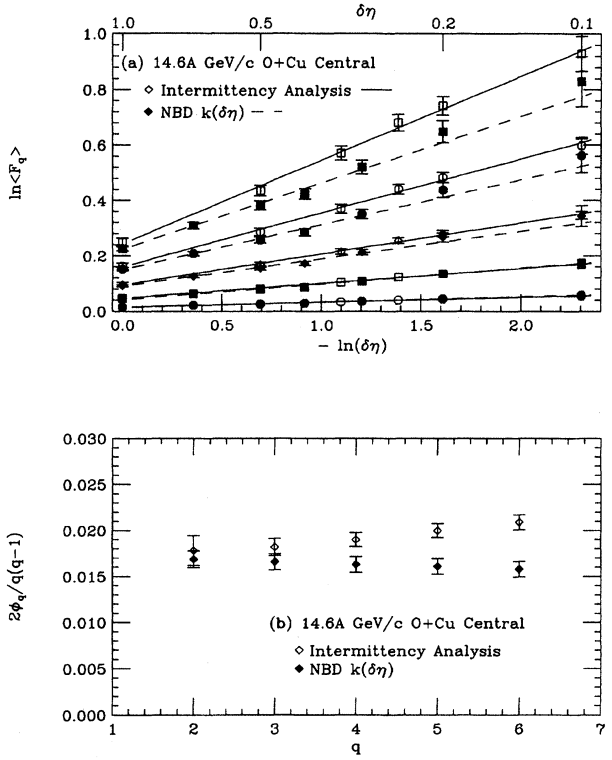

FIG. 8. (a) Normalized factorial moments F_q for central collisions of ^{16}O+Cu, for orders $q=2,3,4,5,6$, from the intermittency analysis Fig. 1(a) (open points) compared to the same quantities computed from the NBD parameter $k(\delta\eta)$ of Fig. 6(a) (solid points), with lines as in Fig. 1(a). (b) Power-law slopes ϕ_q in the scaling form $2\phi_q/q(q-1)$ from the intermittency analysis Fig. 1(b) (open points) compared to the computation from the NBD parameter $k(\delta\eta)$ (solid points).

It is now possible to relate the directly measured evolution of the fluctuations of multiplicity with increasing pseudorapidity interval—as described in terms of the negative binomial distributions which excellently fit the measurements—to the normalized factorial moment analysis of the same data. The strikingly linear evolution of the NBD parameter $k(\delta\eta)$ with the width of the interval explains the observation of power laws based on the intermittency formalism in a much more simple, elegant, and understandable way. The apparent power laws with fractional exponent are simply an artifact of using the quantity F_2-1, which is the inverse of a linear quantity $k(\delta\eta)$ [47]. The intermittency phenomenology, which looks for self-similar fluctuations at all scales $\delta\eta$ by a power-law increase of bin-averaged normalized factorial moments with decreasing bin size $\delta\eta$, obscures the underlying physics of multiplicity fluctuations, which is given simply and elegantly by the linear evolution of $k(\delta\eta)\equiv 1/(F_2-1)$.

Furthermore, for all orders of the normalized factorial moments measured in this experiment (Fig. 1) the apparent power-law increase with decreasing bin size $\delta\eta$ is entirely given by the negative binomial distribution best fit curves, represented by the single parameter $k(\delta\eta)$—and has nothing to do with the derivations of the measured data points from the best fit curves [48,49]. The normalized factorial moments of all orders can be obtained from the single parameter $k(\delta\eta)$ of the NBD fit [see Eq. (8)], and compared point by point with the results of the moment analysis up to sixth order [see Fig. 8(a)]. The low order moments agree to well within the statistical errors (see Table III), but there appears to be a small systematic discrepancy between the two methods, which increases slightly with increasing order and which is clearly evident in the slope parameters [Fig. 8(b)]. Part of the discrepancy may come from the slight difference

TABLE III. Comparison of NBD fits to normalized factorial moment analysis.

$\delta\eta$	$\langle n\rangle,(\sigma)$ Data	$\mu,(\sigma)$ Fit	k Fit	$1/(F_2-1)$ Moment analysis
0.1	2.69 (1.53)	2.41 (1.66)	16.35±1.7	17.68±1.2
0.2	4.92 (2.40)	4.86 (2.44)	21.37±1.3	22.38±1.9
0.5	11.84 (3.96)	11.84 (3.94)	37.52±1.6	36.80±5.0
1.0	22.63 (5.53)	22.60 (5.53)	64.43±2.5	63.98±14.8

in the actual data for the two methods (except for the $\delta\eta = 1.0$ interval as noted above) and may therefore be real. It is also conceivable [50] that the NBD fits, which give excellent values for the low order moments with the best statistics, may give smooth values for the high order moments, which miss the fluctuations of the data points at high multiplicity seemingly indicated in Figs. 2 and 5 [51]. Two comments are relevant on this possibility: The only visible fluctuations of the data from the curves occur for $n \geq 15$ (and therefore are relevant only for the 15th moment or higher); because of the excellence of the χ^2 of the fits, these fluctuations (as noted above) are consistent with *statistical fluctuations*. In any case, the slight differences in the results of the two methods would not affect the fractal interpretation of either set of data points in Fig. 8, presented in the factorial moment formalism of intermittency.

It is also rather instructive to compare the results of the NBD fit for $k(\delta\eta)$ in the present analysis to our previous vertical moment computation [13] of $1/(F_2-1)$ for the $\delta\eta = 1.0$ interval, which should be identical since the data are identical and since the first two moments obtained from the data and the fit are identical (see Table III)—the values agree, but the quoted errors differ by a factor of 6. The errors and best fit values for the NBD fits were checked by comparison to the formula [Eq. (9)] and by fitting published data from NA35 [52,53]. The anomalous error quoted for the moment analysis [13] is testimony to the confusion inherent in that method.

One trivial computational problem is the formulation in terms of the normalized factorial moments, which are unity for the Poisson distribution, rather than in terms of the normalized factorial cumulants [39] (see below), which are zero. Thus slight deviations from Poisson would show up directly as the leading term in the cumulants, but are small compared to the leading 1.0 in the normalized factorial moment computations. Another superior property of factorial cumulants [39,40] compared to factorial moments is that the factorial cumulants are additive for statistically independent subpopulations [42]. Of course, the principal advantage of moment analyses is that they work independently of whether the data happen to be in the form of a convenient distribution.

VIII. CORRELATIONS AND MUELLER MOMENTS

Correlations were known to play an important role in multiplicity distributions since the early 1970s. One of the important conceptual breakthroughs was the realization, by Mueller [39], that the distribution of multiplicity for multiple particle production would not be Poisson unless the particles were emitted independently, without any correlation, but that short-range rapidity correlations were expected as a consequence of "Regge-Pole-dominated" reactions. The non-Poisson distribution of multiplicity and short-range rapidity correlations were observed and well documented [15].

Mueller [39] introduced a series of moments and correlation functions to describe multiparticle correlations. The Mueller moments, or unnormalized factorial cumulants [39,40,42], $f_q \equiv \langle n \rangle^q K_q$, are the integrals of the Mueller correlation functions C_q on an interval, just as the unnormalized factorial moments are the integrals of the q-particle rapidity densities $\rho_q(y_1, \ldots, y_q)$ on the interval. Both K_q and C_q are zero if there is no direct q-particle correlation [54,55]. The most straightforward Mueller correlation function is for two particles,

$$C_2(y_1,y_2) = \rho_2(y_1,y_2) - \rho_1(y_1)\rho_1(y_2), \tag{15}$$

which obviously vanishes for the case of no correlation where $\rho_2(y_1,y_2) = \rho_1(y_1)\rho_1(y_2)$. The two-particle correlation is also expressed in the reduced or normalized form

$$R(y_1,y_2) = \frac{C_2(y_1,y_2)}{\rho_1(y_1)\rho_1(y_2)} = \frac{\rho_2(y_1,y_2)}{\rho_1(y_1)\rho_1(y_2)} - 1, \tag{16}$$

and the two-particle correlation function used for the study of quantum-statistical (Hanbury-Brown Twiss) correlations [56] is

$$r_2(y_1,y_2) = \frac{\rho_2(y_1,y_2)}{\rho_1(y_1)\rho_1(y_2)} = R(y_1,y_2) + 1. \tag{17}$$

IX. TWO-PARTICLE CORRELATIONS, THE NBD, AND INTERMITTENCY

The importance of two-particle correlations to completely determine the multiplicity distribution was pointed out by Fowler and Weiner [9], and more recently by Giovannini and Van Hove [16]. The application of two-particle short-range correlations to the intermittency phenomenology was pioneered by Carruthers *et al.* [17], Capella, Fialkowski, and Krzywicki [18], and Carruthers and Sarcevic [19]. The reduced two-particle short-range correlation [Eq. (16)] is parametrized in an exponential form

$$R(y_1,y_2) = R(0,0)e^{-|y_1-y_2|/\xi}, \tag{18}$$

where ξ is the correlation length. Then, if the inclusive single-particle density $\rho_1(y)$ is taken to be constant, the integral of $C_2(y_1,y_2)$ on an interval of full width $\delta\eta$, $0 \leq y_1 \leq \delta\eta$, $0 \leq y_2 \leq \delta\eta$, can be easily performed to obtain

$$K_2 \equiv F_2 - 1 = \frac{\int^{\delta\eta} dy_1 dy_2 C_2(y_1,y_2)}{\langle n(\delta\eta)\rangle^2} = R(0,0)\frac{[1-(\xi/\delta\eta)(1-e^{-\delta\eta/\xi})]}{\delta\eta/2\xi}. \tag{19}$$

For a negative binomial distribution, substitution of the identity $k \equiv 1/(F_2-1)$ into Eq. (19) yields the equation for the evolution of the NBD parameter $k(\delta\eta)$:

$$k(\delta\eta) = \frac{1}{F_2-1} = \frac{1}{R(0,0)}\frac{\delta\eta/2\xi}{[1-(\xi/\delta\eta)(1-e^{-\delta\eta/\xi})]}. \tag{20}$$

Thus, if it is known (e.g., from the data) that the multiplicity distribution is negative binomial, then the two-particle short-

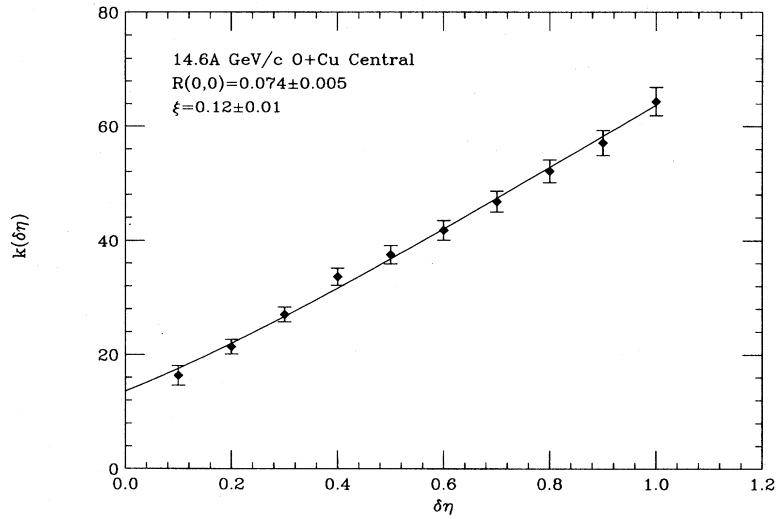

FIG. 9. NBD parameter $k(\delta\eta)$ as a function of the interval $\delta\eta$ [Fig. 6(a)], together with a fit to Eq. (20) with the parameters indicated (solid line).

range correlation determines the entire distribution, including its evolution with $\delta\eta$. Of course, independently of the distribution, Eq. (19) is valid for the evolution of F_2-1 with $\delta\eta$ [57]. Note that Giovannini and Van Hove [16] were the fit to give the relationship between NBD k parameter and the integral of the two-particle correlation function C_2, and a similar derivation was given by De Wolf [58].

Equation (20) represents a mathematical description of the observation that the linear increase of k with $\delta\eta$ is an indication of the randomness of the multiplicity in adjacent $\delta\eta$ bins, while the constancy of k with increasing $\delta\eta$ would be an indication of 100% correlation. In the limit $\delta\eta \ll \xi$, when the $\delta\eta$ interval is well inside the correlation length, $k(\delta\eta)=1/R(0,0)$, a constant. In the limit $\delta\eta \gg \xi$, k is directly proportional to $\delta\eta$, $k(\delta\eta)\simeq\delta\eta/2\xi$, as expected from convolutions of independent bins [17].

The measured evolution of $k(\delta\eta)$, which appears to be strikingly linear, is equally well described by a fit to Eq. (20) (see Fig. 9) which indicates a weak correlation strength $R(0,0)=0.074\pm0.005$ and a very short rapidity correlation length $\xi=0.12\pm0.01$. The correlation length derived from the fit is much shorter than the value $\xi\sim1-3$ for hadron collisions [15]. However, since fits of Eq. (19) to UA5 and other hadron data give parameters which reproduce the directly measured correlations very well [19], there is no reason to doubt the results of the present fit. Thus the present data from O+Cu central collisions can be analyzed within the mainstream two-particle correlation phenomenology of the past decades of multiparticle physics—the difference is merely quantitative, a dramatic reduction of the two-particle correlation length. Intermittency, in central O+Cu collisions, is nothing more than the apparent statistical independence of the multiplicity in rapidity bins of size $\delta\eta\sim0.2$ due to the surprisingly short two-particle rapidity correlation length. The "large" bin-by-bin fluctuations on individual event rapidity distributions from Si+AgBr interactions in cosmic rays [3,59] and the linear evolution of $k(\delta\eta)$ for the present data are both explained by this effect.

X. CORRECTION FOR INSTRUMENTAL EFFECTS

The explanation of the observed intermittency signal by a very-short-range correlation clarifies why various experiments have resorted to studying small volumes in multidimensional phase space to enhance the effect [52,60,61]. The same argument makes the susceptibility to instrumental effects evident—any short-range two-particle correlation generated by the detector mimics the effect, e.g., electronic cross talk [13], Dalitz and external conversions ($\gamma\rightarrow e^+ + e^-$), [61–63] "ghost tracks" (double measurements of the same track [61–63]), etc. In fact, there is a large instrumental short-range correlation in the present data, which further confirms the explanation of intermittency—the present uncorrected data have a known instrumental short-range correlation [13] which produces an intermittency signal that constitutes about half the measured effect.

A short-range correlation was inadvertently built into the detector used for these measurements, since, as noted above, the TMA was constructed of individual small panels which were slightly tilted to avoid inefficiency due to the walls of the tubes. The inefficiency was compensated by a small amount of cross counting on adjacent pads for particles which cross from one wire to another across a tube wall—a built-in short-range correlation. The effect of such cross counting and other cross talk was studied with test beam data, by extensive Monte Carlo (MC) simulations and, finally, by measurement *in situ*. By use of the event simulator Fritiof [64], MC samples having the same number of events as the data were generated. Dalitz decay of π^0 was added to Fritiof and the output was fed through the GEANT package to simulate the detector response and secondary physical effects such as multiple scattering, γ conversions, and particle decays. The GEANT output, which is a list of struck pads, was then analyzed after discarding malfunctioning pads just as in the real data.

The response of the detector to instrumental cross talk, including the small amount of cross talk over tube boundaries, was determined by measuring the ratio of two-pad clusters on adjacent wires *in situ*—using the whole detector and the full data sample. The measured rate at which pads on adjacent wires fired was $(7.45\pm0.11)\%$, which was larger than the predicted rate of $(3.4\pm0.3)\%$ from the MC simulations, which included all the physical (conversions, decays, multiple scattering) and geometrical effects (except for the

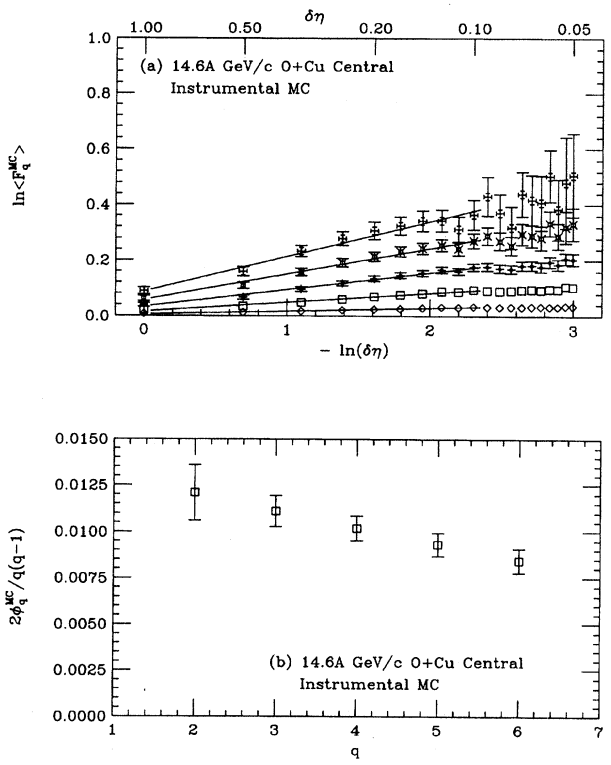

FIG. 10. The final MC results for the instrumental effect, presented in the form of Fig. 1: (a) normalized factorial moments, F_q^{MC}, for orders $q=2,3,4,5,6$; (b) the power-law slopes ϕ_q^{MC} in the form of the scaling law $2\phi_q^{\mathrm{MC}}/q(q-1)$.

slight tilt).[1] The difference of 4% was therefore incorporated into the final Monte Carlo simulation to represent the effect of all cross talk including cross counting.[2]

The results of the final MC simulation for instrumental effects, F_q^{MC}, are presented in Fig. 10, while in Fig. 11, $F_2^{\mathrm{MC}}-1\equiv K_2^I$ is shown together with the measured F_2 moments from ^{16}O+Cu. It can be seen from these plots that the MC simulation also exhibits the characteristic intermittency effect—a power-law increase of F_q^{MC} as the bin size $\delta\eta$ is reduced—but at roughly only half of the measured $\ln(F_q)$ and slope ϕ_q of the data [13]. The instrumental MC simulation can be made to fully reproduce the measured F_q moments by increasing the assumed cross talk to $(8.2\pm0.7)\%$, which is significantly larger than the measured value of $(4.0\pm0.4)\%$. This indicates that there is a net intermittency effect in the data of more than five standard deviation significance. As already described, the conservative counting convention was used for two adjacent pads in the same tube, and the measured cross talk over tube boundaries was explicitly included in the final MC simulation. Thus the net intermittency effect in the data comes from sources other than γ conversions, Dalitz decays, and instrumental cross talk, which are the main contributors to the MC signal because Fritiof gives Poisson distributions [65] and does not exhibit any intermittency, i.e., $F_q^{\mathrm{Fritiof}}(\delta\eta)=1.000\pm0.003$ for all q.

For the normalized factorial moment analysis [13], the measured values of F_q were corrected for instrumental effects by subtracting ΔF_q^I, as determined by the Monte Carlo simulation: $\Delta F_q^I\equiv F_q^{\mathrm{MC}}-F_q^{\mathrm{input}}$, where F_q^{MC} is given in Fig. 10(a) and $F_q^{\mathrm{input}}=1.000$ as noted. To correct the results of the negative binomial distribution analysis, the results of $K_2^I\equiv F_2^{\mathrm{MC}}-1=\Delta F_2^I$ (Fig. 11) for the instrumental effects were first fit [66] to Eqs. (18), (19), which gave an excellent representation (solid curve in Fig. 11) with parameters $R^I(0,0)=0.050\pm0.010$ and $\xi=0.072\pm0.020$. This is, in fact, a reasonable mathematical description of the built-in short-range correlation of the detector,[3] which leads to further confidence that a very-short-range pseudorapidity correlation also explains the intermittency effect in the corrected data.

The correction of the NBD analysis for instrumental effects is then performed by taking the measured two-particle correlation $R(y_1,y_2)$ to be the sum of a true effect plus the instrumental effect:

$$R(y_1,y_2)=R^T(y_1,y_2)+R^I(y_1,y_2), \tag{21}$$

with the further assumption that the instrumental effect has minimal influence on the observed $\langle n(\delta\eta)\rangle$. It then immediately follows from Eqs. (19), (20) that the measured $K_2(\delta\eta)=1/k(\delta\eta)$ is just the sum of the integrals of the true plus the instrumental terms or

$$K_2(\delta\eta)=\frac{1}{k(\delta\eta)}=K_2^T(\delta\eta)+K_2^I(\delta\eta). \tag{22}$$

The true effect $K_2^T(\delta\eta)$ is then simply

$$K_2^T(\delta\eta)=\frac{1}{k(\delta\eta)}-K_2^I(\delta\eta), \tag{23}$$

where $K_2^I\equiv F_2^{\mathrm{MC}}-1=\Delta F_2^I$ is taken from the fit (solid curve) in Fig. 11 and $k(\delta\eta)$ is taken from Fig. 6. The statistical errors for $K_2^T(\delta\eta)$ are summed in quadrature from the two terms, where the original [13] error of $K_2^I(\delta\eta)$ (see Fig. 11) has been corrected, at each $\delta\eta$, to correspond to the NBD

[1]The 3.4% rate of pads on adjacent wires firing, calculated from the Fritiof+GEANT Monte Carlo simulation, consists of a random combinatorial effect of 2.3% from the known multiplicity and $dn/d\eta$ distributions, with only 1.1% from conversions and Dalitz pairs. These latter effects are small because both tracks from the pair tend to fall on a single pad and are counted as a single track in the detector.

[2]The additional rate of $(4.0\pm0.4)\%$ measured *in situ* for two-pad clusters on adjacent wires is consistent with being entirely explained by a slight tilt of the detector panels such that the detection inefficiency and cross talk roughly offset each other at probabilities of approximately 3% as measured in a test beam [26].

[3]Note that the $R^I(0,0)=0.050$ from the fit is the same as the instrumental effect of 5.1%, which is composed of 4.0% cross talk and 1.1% Dalitz and conversions. However, the numerical equality is an accident, since to go from the percent cross talk on pads on adjacent wires to $R(y_1,y_2)$ involves normalization [Eq. (16)] by an additional factor of $\rho_1\times\delta\eta$, for the adjacent ring of pads, which is of order unity: $(dn/d\eta\sim23)\times(\delta\eta\sim0.05)\simeq1$.

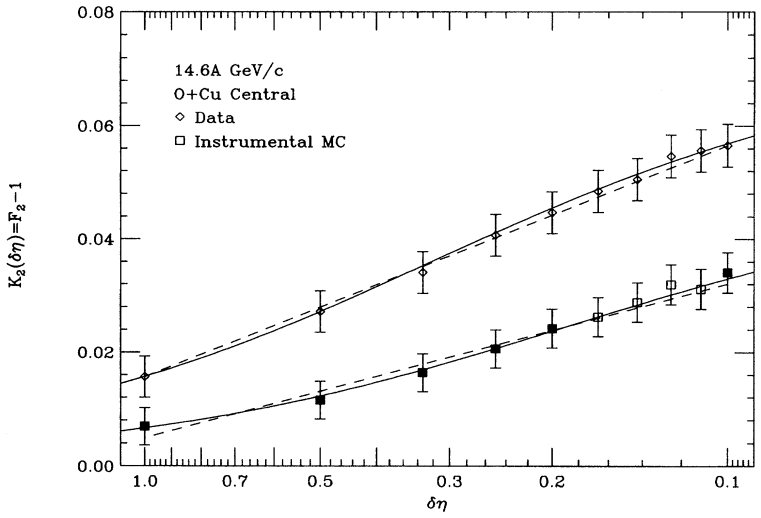

FIG. 11. Instrumental MC result from Fig. 10(a) for $F_2^{\mathrm{MC}}-1\equiv K_2^I$ (squares), together with the measured F_2-1 moments (diamonds) from the ^{16}O+Cu central collision data [Fig. 1(a)], shown on a linear scale, as a function of $\delta\eta$ on a logarithmic scale. The solid line on the data is the fit to $k(\delta\eta)$ from Fig. 9. The solid line on the instrumental MC simulation is a fit to Eq. (19) using the solid points, with errors corrected as noted [66]. The dashed lines on the plot are the power-law fits from the intermittency analyses.

methodology [66]. It is important to note that Eqs. (19), (21), (22) are valid in general, for any distribution, and provide a physical explanation of the method used to correct the E802 normalized factorial moment analysis [13] for instrumental effects.

XI. FINAL RESULTS FOR $R(0,0)$ AND ξ

In keeping with the notation based on the NBD, the final results are quoted as $1/K_2^T(\delta\eta)$, denoted $k^C(\delta\eta)$, and are plotted vs $\delta\eta$ in Fig. 12, which clearly illustrates, again, the simple linear evolution and nonzero intercept. The final values of $R(0,0)$ and ξ, corrected for instrumental effects, are derived from a fit of these data to Eq. (20): $R(0,0)=0.031\pm0.005$, $\xi=0.183^{+0.051}_{-0.042}$ (statistical errors). The systematic error, predominantly from the measured cross-talk uncertainty ($4.0\%\pm0.4\%$), is ±0.003 for $R(0,0)$ and ±0.01 for ξ. These results are consistent with previous attempts at direct measurements of two-particle rapidity correlations in O+emulsion [67] and S+A [68,69,49] central collisions, which also indicate a much weaker correlation strength than hadron collisions, and a reduced rapidity correlation length [69]. The hadron short-range correlation length at low energies is known [15] to be roughly $\xi\sim2$ units of rapidity, with strength $R(0,0)\sim0.6$. Thus, for the weak correlation strength and small correlation length derived from the E802 data to make sense, it must be that the standard hadronic short-range correlation effect is diluted by the multiple collisions in the ^{16}O+Cu reaction. Similar conclusions in the context of the conventional intermittency slope parameters are given in Refs. [17,18,22,23].

It is interesting that exactly the deduced effects from the E802 data—weakened, but finite, short-range rapidity correlations in collisions of relativistic heavy ions—were predicted several years ago [17,18,20,21]. In nucleus-nucleus collisions, the conventional short-range correlations should be washed out by the random superposition of correlated sources [18,22,23], so that eventually only the quantum-statistical Bose-Einstein (BE) correlations should remain [17,18,24]. Other experiments have reported a relationship of intermittency and BE correlations [62,63,65,70]. If BE correlations were the entire effect, then direct measurements of BE correlations in the variable $\delta\eta$, instead of the usual variable [56] ($Q=p_1-p_2$), combined with an estimate of the

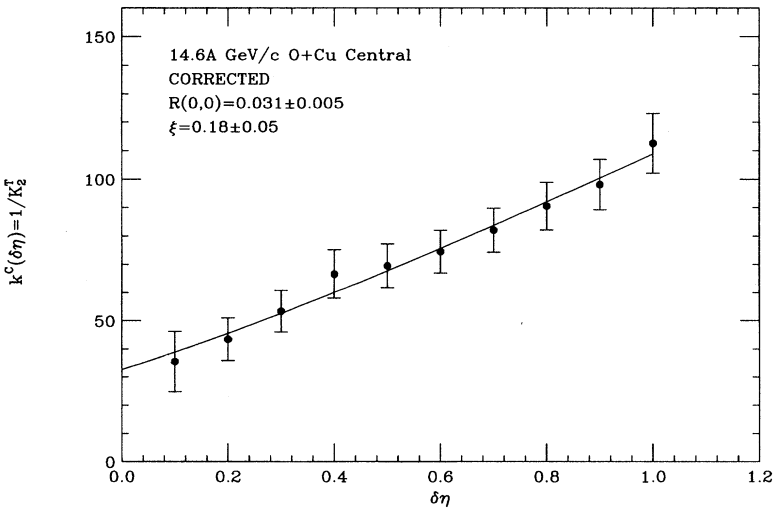

FIG. 12. k parameter from NBD fits to the data, corrected for instrumental effects, as explained in the text, presented as $k^C(\delta\eta)\equiv1/K_2^T(\delta\eta)$ as a function of the interval $\delta\eta$. The solid line is a fit to Eq. (20) with the parameters indicated.

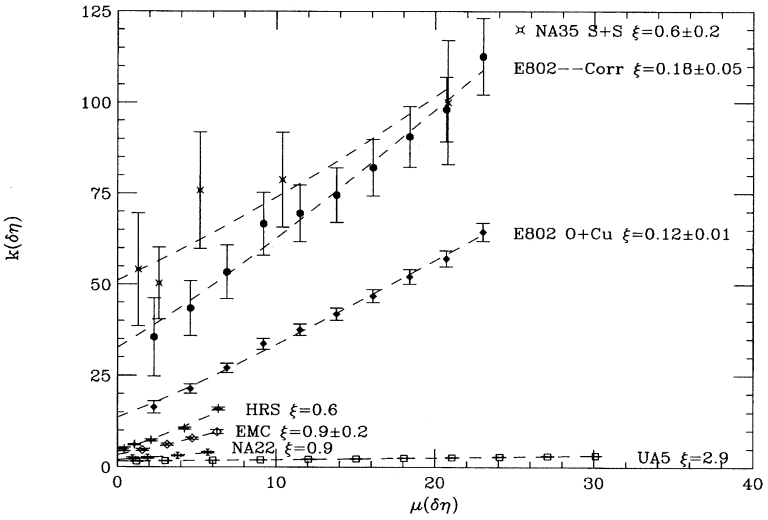

FIG. 13. NBD parameter $k(\delta\eta)$ as a function of the mean multiplicity in the pseudorapidity interval $\mu(\delta\eta)=dn/d\eta\times\delta\eta$: UA5 $\bar{p}+p\sqrt{s}=540$ GeV ($dn/d\eta=3.01$), NA22 $p+p\sqrt{s}=22$ GeV (1.90), EMC μ-p DIS $W=18-20$ GeV (1.57), HRS e^+e^- 2-jet$\sqrt{s}=29$ GeV (2.12), E802 O+Cu central $P_{\rm beam}=14.6A$ GeV/c (23.0), E802 corrected $k^C(\delta\eta)$, NA35 S+S central $E_{\rm beam}=200A$ GeV (10.4). The dashed lines are fits to Eq. (20) with the parameters ξ indicated.

particle composition in the TMA detector from spectrometer results [34], should reproduce the parameters derived from the evolution of $k^C(\delta\eta)$.

XII. RELATED MEASUREMENTS

It is clear that the present E802 data have much in common with the original UA5 [2,5] observation—an increase in the width of the multiplicity distributions about the average with decreasing $\delta\eta$ interval, well fit by the negative binomial distribution. Since the pioneering work of UA5, many other experiments have shown that the NBD provides excellent fits to charged multiplicity distributions in restricted $\delta\eta$ intervals for all reactions studied, for example, $p+p$ (NA22 [71]), e^+e^- (HRS [72]), μ-p DIS (EMC [73]), and S+S central (NA35 [52]). Particularly noteworthy is that all these previously published measurements show the same effect as the present data—linear dependences of the NBD parameter $k(\delta\eta)$ with the pseudorapidity interval $\delta\eta$ or, equivalently, with the mean multiplicity in the interval $\mu(\delta\eta)$, with nonzero intercept $k(0)\neq 0$ (see Fig. 13). However, the present data (and also to a certain extent, the other heavy ion data, NA35 S+S) are quantitatively, rather than qualitatively, different from the others in that $k(\delta\eta)$ is much larger and the dependence on $\delta\eta$ much steeper. As previously noted, fits of Eq. (20) to the hadron data give values for ξ and $R(0,0)$ which reproduce the directly measured correlations very well [19]. These fits are shown by dashed lines in Fig. 13. The difference between the present and previous data is merely quantitative: The rapidity correlation length is $\xi\sim 3$ in UA5, $\xi\sim 0.2$ in E802.

There is some other previous work on NBD fits as a function of pseudorapidity interval in relativistic heavy ion collisions. Two emulsion experiments have presented NBD fits to minimum bias multiplicity distributions in ^{16}O and ^{28}Si reactions [43,74], with limited statistics (≤ 1000 events). Of course, minimum bias distributions look nothing like those in Figs. 2 and 4, and furthermore, the fluctuations are more dominated by nuclear geometry and the various target components than by fundamental hadron dynamics. NBD fits to multiplicity distributions in central ^{32}S+A collisions at 200A GeV have been presented by two experiments: EMU01 [75] with ~ 350 events for S+Au, and NA35 [52] with 2856 events for S+S collisions and 270 events for S+Au. Interestingly, both experiments find excellent fits to the NBD in S+Au collisions, but their results for $k(\delta\eta)$ disagree. Multiplicity distributions with a zero degree calorimeter centrality cut, but without fits, were presented by another AGS experiment [76] at 14.6A GeV/c for ^{28}Si+Al,Cu,Pb, for a fixed pseudorapidity interval $\delta\eta\simeq 0.6$, as a function of the position of the center of the interval. The distributions show fluctuations that favor high multiplicity, but do not change shape as the center of the interval is varied from $\eta=1.1-3.5$, except for the most forward position.

Of most importance for the comparison to the present measurement is the high statistics NA35 S+S data, with centrality cut (2.6%) made by a zero degree calorimeter, where the result for $k(\delta\eta)$ was shown in Fig. 13. It is instructive to try to understand the precision obtained for the NBD parameter $k(\delta\eta)$ from the two heavy ion experiments, NA35 and the present experiment, E802. The error estimate $s_{1/k}$ for the NBD parameter $1/k$ was given above [Eq. (9)]. Thus, to an excellent approximation, the required number of events, N, for a fixed percent error in s_k/k, is

$$N=2\frac{k^2}{\mu^2}\left(\frac{k}{s_k}\right)^2. \tag{24}$$

This explains why the errors for NA35 S+S with 2856 events are so much larger than E802 O+Cu with 19 667 events—(k/μ) is 2–3 times larger—even though NA35, in distinction to all the other NBD fit experiments, combined the data from all intervals of a given size (as in the normalized factorial moment analysis) to reduce the errors. Interestingly, the fit of Eq. (20) to the NA35 data, shown as the dotted line in Fig. 13 with $\xi=0.6^{+0.4}_{-0.2}$, indicates that k increases with $\delta\eta$ (i.e., $1/\xi\neq 0$) to 99.4% confidence (2.5σ), which is somewhat in disagreement with the conclusions reached by NA35 from these data [52], and also by EMU01 [75], that "the NBD parameter ($1/k$) is (within the errors) independent of the width of the rapidity interval." Of course,

the present measurement, corrected for instrumental effects, gives a much clearer (3.5σ) effect for the variation of $k(\delta\eta)$.

XIII. SUMMARY AND CONCLUSIONS

E802 ^{16}O+Cu central (ZCAL) multiplicity distributions in bins of pseudorapidity $\delta\eta=0.1,0.2,\ldots,1.0$ show an apparent fractional power-law growth of normalized factorial moments with decreasing pseudorapidity interval, in agreement with previous intermittency analyses. The same data also exhibit excellent fits to negative binomial distributions. Consequently, the present data allow for the first time a comprehensive formulation of the subject of intermittency in terms of distributions to complement the analysis based on moments. Of course, many of the individual components of the present analysis have been noted by previous authors [9,16–24,58,62,63,65,70,77–79].

In agreement with all previous measurements of NBD fits to multiplicity distributions in hadron and lepton reactions, the k parameter of the NBD fit for central ^{16}O+Cu collisions is found to exhibit an apparently linear increase with the $\delta\eta$ interval and a nonzero intercept $k(0)\neq 0$. The heavy ion data are quantitatively rather than qualitatively different from the others in that $k(\delta\eta)$ is much larger and the dependence of $\delta\eta$ much steeper. The evolution of the NBD parameter $k(\delta\eta)$ is used to determine the two-particle short-range rapidity correlation length for central ^{16}O+Cu collisions, $\xi=0.18\pm0.05$, which, although much shorter than the value $\xi\sim 1-3$ for hadron collisions, is clearly nonzero. True intermittency—a scale-invariant power-law singularity as $\delta\eta\rightarrow 0$—would correspond [80] to the limit $\xi\rightarrow 0$, which can only occur if the intercept $k(0)\rightarrow 0$. In this case, $K_2=1/k$ would obviously diverge as $\delta\eta\rightarrow 0$, and the non-Poisson multiplicity distributions in small $\delta\eta$ bins would, in fact, be fully statistically independent—a clear example of a singular correlation. However, this is not observed in any experiment. There is no doubt that the correlation length remains finite for the present data, since $k(0)=32.7\pm5.4(\text{stat})\pm2.4(\text{syst})$ differs from zero by huge statistical significance, implying that there really is a two-particle correlation with very small correlation length and, therefore, no intermittency.

ACKNOWLEDGMENTS

This work has been supported by the U.S. Department of Energy under contracts with ANL (W-31-109-ENG-38), BNL (DE-AC02-76CH00016), Columbia University (DE-FG02-86-ER40281), LLNL (W-7405-ENG-48), MIT (DE-AC02-76ER03069), UC Riverside (DE-FG03-86ER40271), and NASA (NGR-05-003-513), under contract with the University of California, and by the U.S.–Japan High Energy Physics Collaboration Treaty. The flawless operation of the Tandem-AGS facility at BNL is appreciated. Discussions and/or correspondence with P. Carruthers, G. Ekspong, R. Hwa, I. Otterlund, D. Seibert, N. Tannenbaum, and R. Weiner are acknowledged. V. Cianciolo provided a critical reading of the manuscript.

[1] A. Bialas and R. Peschanski, Nucl. Phys. **B273**, 703 (1986); **B308**, 847 (1988).

[2] J. G. Rushbrooke, contribution 6th High Energy Heavy Study (Berkeley, 1983); P. Carlson, in Proceedings of the 4th Workshop on $\bar{p}$-p Collider Physics, Bern, 1984, CERN Yellow Report No. 84-09, 1984; UA5 Collaboration, G. J. Alner *et al.*, Phys. Lett. **138B**, 304 (1984).

[3] JACEE Collaboration, T. H. Burnett *et al.*, Phys. Rev. Lett. **50**, 2062 (1983).

[4] B. B. Mandelbrot, *The Fractal Geometry of Nature* (Freeman, New York, 1983).

[5] UA5 Collaboration, G. J. Alner *et al.*, Phys. Lett. **160B**, 193 (1985); see also UA5 Collaboration, G. J. Alner *et al.*, Phys. Rep. **154**, 247 (1987), and references therein.

[6] P. Carruthers and C. C. Shih, Phys. Lett. **127B**, 242 (1983); **165B**, 209 (1985). See also Ekspong [7].

[7] G. Ekspong, in *Festschrift for Leon Van Hove and Proceedings Multiparticle Dynamics*, edited by A. Giovannini and W. Kittel (World Scientific, Singapore, 1990), and references therein.

[8] W. Thome *et al.*, Nucl. Phys. **B129**, 365 (1977); see also K. Eggert *et al.*, *ibid.* **B86**, 201 (1975).

[9] G. N. Fowler and R. M. Weiner, Phys. Lett. **70B**, 201 (1977); Phys. Rev. D **17**, 3118 (1978); Nucl. Phys. **A319**, 349 (1979); Phys. Rev. D **37**, 3127 (1988).

[10] G. N. Fowler, E. M. Friedlander, and R. M. Weiner, Phys. Lett. **104B**, 239 (1981).

[11] L. Van Hove, Physica **147A**, 19 (1987); see also L. Van Hove, Phys. Lett. B **232**, 509 (1989).

[12] See, for example, M. J. Tannenbaum, Int. J. Mod. Phys. A **4**, 3377 (1989), and references therein.

[13] E802 Collaboration, T. Abbott *et al.*, Phys. Lett. B **337**, 254 (1994).

[14] For an extensive review of this work, see A. Bialas, Nucl. Phys. **A525**, 345c (1991).

[15] E.g., see L. Foa, Phys. Rep. C **22**, 1 (1975); J. Whitmore, *ibid.* **27**, 187 (1976); **10**, 273 (1974); H. Boggild and T. Ferbel, Annu. Rev. Nucl. Sci. **24**, 451 (1974).

[16] A. Giovannini and L. Van Hove, Z. Phys. C **30**, 391 (1986).

[17] P. Carruthers, E. M. Friedlander, C. C. Shih, and R. M. Weiner, Phys. Lett. B **222**, 487 (1989).

[18] A. Capella, K. Fialkowski, and A. Krzywicki, in *Festschrift for Leon Van Hove and Proceedings Multiparticle Dynamics*, edited by A. Giovannini and W. Kittel (World Scientific, Singapore, 1990); Phys. Lett. B **230**, 149 (1989).

[19] P. Carruthers and Ina Sarcevic, Phys. Rev. Lett. **63**, 1562 (1989); Ina Sarcevic, Nucl. Phys. **A525**, 361c (1991); P. Carruthers, H. C. Eggers, and Ina Sarcevic, Phys. Lett. B **254**, 258 (1991); P. Carruthers *et al.*, Int. J. Mod. Phys. A **6**, 3031 (1991).

[20] K. L. Wieand, S. E. Pratt, and A. B. Balantekin, Phys. Lett. B **274**, 7 (1992).

[21] D. Seibert, Phys. Rev. C **47**, 2320 (1994).

[22] P. Lipa and B. Buschbeck, Phys. Lett. B **223**, 465 (1989).
[23] D. Seibert, Phys. Rev. D **41**, 3381 (1990).
[24] M. Gyulassy, in *Festschrift for Leon Van Hove and Proceedings Multiparticle Dynamics*, edited by A. Giovannini and W. Kittel (World Scientific, Singapore, 1990), p. 479.
[25] T. Abbott *et al.*, Nucl. Instrum. Methods A **290**, 41 (1990).
[26] T. Abbott, Ph.D. thesis, University of California at Riverside, 1990.
[27] D. Beavis *et al.*, Nucl. Instrum. Methods A **281**, 367 (1989).
[28] L. Remsberg *et al.*, Z. Phys. C **38**, 35 (1988).
[29] EMU01 Collaboration, M. Adamovich *et al.*, Phys. Rev. Lett. **65**, 412 (1990).
[30] R. Holynski *et al.*, Phys. Rev. Lett. **62**, 733 (1989).
[31] I. V. Ajinenko *et al.*, Phys. Lett. B **222**, 306 (1989).
[32] EMU01 Collaboration, M. Adamovich *et al.*, Phys. Lett. B **263**, 539 (1991).
[33] Thanks to J. A. Appel of Fermilab for bringing this to our attention.
[34] E-802 Collaboration, T. Abbott *et al.*, Phys. Rev. C **50**, 1024 (1994).
[35] Of course, the intermittency analysis depends on the evolution of the moments and distributions with $\delta\eta$, and it is not at all clear how a distortion due to a sharp cut would affect that analysis.
[36] R. D. Evans, *The Atomic Nucleus* (McGraw-Hill, New York, 1955).
[37] A. C. Melissinos, *Experiments in Modern Physics* (Academic, New York, 1966).
[38] H. Jeffreys, *Theory of Probability* (Clarendon, Oxford, 1961).
[39] A. H. Mueller, Phys. Rev. D **4**, 150 (1971).
[40] M. G. Kendall and A. Stuart, *The Advanced Theory of Statistics* (Hafner, New York, 1969).
[41] E.g., see A. Bialas and R. Peschanski, Phys. Lett. B **207**, 59 (1988).
[42] P. Carruthers and C. C. Shih, Int. J. Mod. Phys. A **2**, 1447 (1987); P. Carruthers, *ibid.* **4**, 5587 (1989).
[43] EMU01 Collaboration, M. I. Adamovich *et al.*, Phys. Lett. B **242**, 512 (1990).
[44] WA80 Collaboration, R. Albrecht *et al.*, Z. Phys. C **45**, 31 (1989).
[45] See W. Q. Chao, T. C. Meng, and J. C. Pan, Phys. Lett. B **176**, 211 (1986).
[46] S. Uhlig *et al.*, Nucl. Phys. **B132**, 15 (1978).
[47] Interestingly, this is essentially the exact opposite of the philosophy of B. Buschbeck, P. Lipa, and R. Peschanski, Phys. Lett. B **215**, 788 (1988).
[48] This is rather different from the recent data of the WA80 Collaboration [49] in which deviations from a NBD fit to peripheral Si+Au collisions are clearly not statistical and where F_5 from the NBD fit is a factor of 3 smaller than the direct calculation.
[49] R. Albrecht *et al.*, Phys. Rev. C **50**, 1048 (1994).
[50] R. C. Hwa and J. C. Pan, Phys. Rev. D **46**, 2941 (1992).
[51] Of course the gamma distribution fits which give the same conclusions as the NBD fits are all higher than the data points at high multiplicity.
[52] NA35 Collaboration, J. Bächler *et al.*, Z. Phys. C **57**, 541 (1993).
[53] Thanks to Ivo Derado and Barbara Wosiek for supplying a listing of the data points.
[54] Note that the Mueller moments f_q go to zero trivially in the limit $\langle n\rangle \to 0$, so that the normalized factorial cumulants K_q must be used to test for direct q-particle correlations in this limit [55].
[55] See, for instance, W. Bell *et al.*, Z. Phys. C **22**, 109 (1984).
[56] For recent reviews, see B. Lorstad, Int. J. Mod. Phys. A **4**, 2861 (1988); W. A. Zajc, in *Hadronic Multiparticle Production*, edited by P. Carruthers (World Scientific, Singapore, 1988).
[57] Note that a formula given in Ref. [19] gives identical results to Eq. (19) in both limits and is virtually indistinguishable over the whole range.
[58] E. A. De Wolf, Acta Phys. Pol. B **21**, 611 (1990).
[59] M. J. Tannenbaum, Mod. Phys. Lett. A **9**, 89 (1994).
[60] KLM Collaboration, R. Holynski *et al.*, Phys. Rev. C **40**, R2449 (1989); W. Ochs and J. Wosiek, Phys. Lett. B **214**, 617 (1988); see also EHS/NA22 Collaboration, I. V. Ajinenko *et al.*, *ibid.* **235**, 373 (1990).
[61] EMU01 Collaboration, M. I. Adamovich *et al.*, Nucl. Phys. **B388**, 3 (1992).
[62] I. Derado, G. Jancso, and N. Schmitz, Z. Phys. C **56**, 553 (1992).
[63] NA35 Collaboration, J. Bächler *et al.*, Z. Phys. C **61**, 551 (1994); see also NA35 Collaboration, P. Seyboth *et al.*, in *Proceedings of Hadron Structure'92, Stara Lesna, Czecho-Slovakia*, edited by D. Bruncko and J. Urban (Institute of Experimental Physics, Kosice, 1992).
[64] B. Nilsson-Almqvist and E. Stenlund, Comput. Phys. Commun. **43**, 387 (1987).
[65] K. Kadija and P. Seyboth, Phys. Lett. B **287**, 363 (1992).
[66] The original MC error, which is the same for all points, $\sigma_{K_2^l(\delta\eta)}=0.0034$ (Fig. 11), is divided by an empirical factor of $6\times\delta\eta$, which brings the errors of the two methods from Table III into agreement.
[67] KLM Collaboration, H. von Gersdorff *et al.*, Phys. Rev. C **39**, 1385 (1989).
[68] E814 Collaboration, J. Barrette *et al.*, Phys. Rev. C **49**, 1669 (1994).
[69] EMU01 Collaboration, R. J. Wilkes *et al.*, Nucl. Phys. **A544**, 153c (1992).
[70] EHS/NA22 Collaboration, I. V. Ajinenko *et al.*, Z. Phys. C **61**, 567 (1994).
[71] EHS/NA22 Collaboration, M. Adamus *et al.*, Z. Phys. C **37**, 215 (1988); Phys. Lett. B **177**, 239 (1986).
[72] HRS Collaboration, M. Derrick *et al.*, Phys. Lett. **168B**, 299 (1986); Phys. Rev. D **34**, 3304 (1986).
[73] EMC Collaboration, M. Arnedo *et al.*, Z. Phys. C **35**, 335 (1987).
[74] P. L. Jain, A. Mukhopadhyay, and G. Singh, Phys. Lett. B **294**, 27 (1992).
[75] EMU01 Collaboration, M. I. Adamovich *et al.*, Z. Phys. C **56**, 509 (1992).
[76] E814 Collaboration, J. Barrette *et al.*, Phys. Rev. C **46**, 312 (1992).
[77] I. M. Dremin, Sov. Phys. Usp. **33**, 647 (1990).
[78] S. Barshay, Z. Phys. C **47**, 199 (1990).
[79] T. Awes, "Koba-Nielsen-Olesen Scaling, Intermittency, and Statistics," ORNL Physics Division report, 1990 (unpublished).
[80] M. J. Tannenbaum, Phys. Lett. B **347**, 431 (1995).